Accepted Manuscript

Transverse impact response of filament wound basalt composite tubes

Iqbal Mokhtar, Mohd Yazid Yahya, Ab Saman Abd Kader, Shukur Abu Hassan, Carlo Santulli

PII: S1359-8368(17)30049-5

DOI: 10.1016/j.compositesb.2017.01.005

Reference: JCOMB 4816

To appear in: *Composites Part B*

Received Date: 13 December 2015

Revised Date: 16 November 2016

Accepted Date: 5 January 2017

Please cite this article as: Mokhtar I, Yahya MY, Abd Kader AS, Hassan SA, Santulli C, Transverse impact response of filament wound basalt composite tubes, *Composites Part B* (2017), doi: 10.1016/j.compositesb.2017.01.005.

TRANSVERSE IMPACT RESPONSE OF FILAMENT WOUND BASALT COMPOSITE TUBES

Iqbal Mokhtar[1], Mohd Yazid Yahya[1 *], Ab Saman Abd Kader[2], Shukur Abu Hassan[1] and Carlo Santulli[3]

[1] Centre for Composites, Universiti Teknologi Malaysia, 81310 Skudai Johor, Malaysia

[2] Marine Technology Centre, Universiti Teknologi Malaysia, 81310 Skudai Johor, Malaysia

[3]Università degli Studi di Camerino, School of Architecture and Design, viale della Rimembranza, 63100 Ascoli Piceno, Italy

Keywords: A. Polymer matrix composites (PMCs); A. Glass fibres; B. Impact behaviour; E. Filament winding; Basalt tubes

ABSTRACT. The aim of this study was to determine the effect of impact energy and impactor size on basalt filament wound composite tubes with different winding angles. Tubes with four different winding angles $[\pm 45^0]_3$, $[\pm 55^0]_3$, $[\pm 65^0]_3$ and $[\pm 75^0]_3$ were subjected to various impact energy levels, 4, 6, 8 and 10 J, using four different impactor diameters, 6.35, 10, 12.7 and 15.9 mm. The results obtained revealed the significant effect of energy levels, despite the limited range purposely studied. In particular, not only maximum damage diameter (MDD) but also the geometry of damage area is influenced by impact energy. MDD also increases the higher the winding angles. In addition, basalt tubes with higher winding angles absorb less energy than the tubes with

* Corresponding author, e-mail: yazid@fkm.utm.my

smaller winding angles for any given impact energy: this may be also the effect of them being slightly thinner.

Impact damage typically propagates in the fibre direction of the tubes. Impact using larger impactors increases the dimensions of damage area, hence reducing the penetration. In comparison with E-glass tubes with similar amount of reinforcement, damage area of basalt tubes is significantly smaller at all impact energies.

1. INTRODUCTION

Falling weight impact on composite laminates has been widely examined during last decades: most published work has focused on the effect of impact on composite panels, although also the effect of impact on curved structures, such as tubes has been widely investigated. Low velocity transverse impacts are known to cause a number of different damage phenomena, including matrix cracking, delamination, and fibre breakage. It has also been reported that damage in the form of matrix cracks and delamination may often be difficult to detect by the naked eye, since it can be wholly embedded within the thickness of the laminate. This invisible damage is often responsible for the deterioration of the overall strength and stiffness of the laminate [1]. A considerable amount of research has been performed to investigate the behaviour of composite tubes under low velocity impact loads. Deniz *et al.* [2] considered the impact response and axial compression after impact of E-glass/epoxy composite tubes with various diameters (50, 75, 100, and 150 mm) and energy levels (4, 6, 8, and 10 J). They clarified that for E-glass/epoxy composite tubes the maximum contact force increases the higher the impact energy for tubes with smaller diameter, while it does not significantly change for tubes with higher diameter. The study also revealed that tubes

with higher diameters, because of their increased flexibility, absorb more energy elastically and are not damaged as much as the tubes with relatively small diameters for a given impact energy. Deniz and Karakuzu [3] conducted analysis on the effects of seawater absorption on the response of the transversely impacted composite pipes with various diameters. E-glass/epoxy composite pipes were manufactured by filament winding using fibres aligned in the $[\pm 55^{o}]_3$ orientation, and the effects of seawater on impact behaviour for various impact energies were investigated. They performed the experiment within 12 months of continuous exposure to seawater to extract the most reliable results from glass/epoxy tubes in harsh environments. Results indicated that deflection values increase the higher the impact energy for all conditions. Moreover, the already mentioned higher flexibility of tubes with larger diameter has the effect to increase dramatically the delamination area with decreasing diameter of the tubes: in other words, tubes with higher diameter are capable of storing more elastic energy and absorb less energy to failure. Chib [4] performed the low velocity impact simulation of carbon/epoxy tubes using the LS-DYNA software program. His study demonstrated the accuracy and effectiveness of the impact test on tubes with LS-DYNA and the obtained results offered predictions for various parameters, such as impactor velocity, lay-up configuration, and boundary conditions. Doyum and Atalay [5] investigated the detection possibility of different types of defects to produce a result of low velocity transverse impact loading on $(\pm 45_2/90)$ S-glass and $(\pm 54_3/90)$ E-glass fibre-reinforced epoxy tubular specimens. Visual inspection, water-washable red dye, water-washable fluorescent and post-emulsified fluorescent penetrant systems were utilized for damage detection. Damage caused by impact i.e., cracks of different sizes and nature and delamination zones, were detected using non-destructive inspection techniques. The

mechanical properties of basalt composites are comparable with E-glass ones, which should also be the case for impact resistance, although of course the balance of energy, absorbed elastically and plastically, may vary for the two materials. Based on the literature, basalt composites have comparable or slightly higher modulus than E-glass fibres, while both tensile strength and elongation at break are higher [6]. In an overall overview, the use of basalt composites enhanced the environmental sustainability of such composites. The mechanical properties of basalt composite laminates have been reported for both thermoset [7-13] and thermoplastic matrices [14-17]. However, limited attention has been devoted to the impact behaviour of basalt composites [18-24]. Lopresto et al. [18] investigated the mechanical properties and impact response of basalt/epoxy composites, conducting impact tests at energy of 100 Joules to produce the perforation of the laminates. They reported that basalt allowed higher energy absorption when compared to E-glass composites. A series of impact tests have been conducted to investigate the effect on hybrid basalt/E-glass reinforced epoxy composites [10, 25]. They confirmed that basalt exhibits better energy absorption capability when compared to E-glass composites, and they also highlighted that E-glass laminates have comparatively poor damage tolerance. Characteristics of basalt fibre composites can also be enhanced by the application of suitable treatments [26] and good damage tolerance can also be confirmed in the exposure to harsh environments [27].

Sfarra et al. [28] compared the damage features caused by impacts on E-glass and basalt fibre reinforced laminates. The impact test has been assisted by nondestructive interferometric and thermographic techniques that allowed inspecting damage to compare their observations with the results of impact hysteresis cycles. Impact damage observed in basalt fibre reinforced composites was found to be

considerably variable according to the direction of fibres, and was in general slightly superior to that encountered on E-glass laminates: however, directionality may represent a difficulty towards the predictability of the behaviour.

Based on these results, the production of hybrid glass/basalt fibre laminates in different configurations and increased manufacturing complexity will not always provide additional advantage in allowing a better predictability of impact damage patterns. Also the effect of fibre orientation needs to be accounted for: Gideon et al. [29] investigated the responses of basalt unsaturated polyester laminates under static three-point bending and low velocity impact loading. Three types of laminates, unidirectional, cross-ply (0/90) and plain weave, were fabricated by hand lay-up and hot pressing. They mentioned that unidirectional laminate was superior to the others in terms of resistance to static loading, while cross-ply and woven laminates were superior in dynamic loading. The failure of unidirectional laminates occurred along the fibre direction, while damage was localized around the impacted locations for cross-ply and woven laminates. Petrucci et al. [30] evaluated the impact damage characterization of hybrid composite laminates based on basalt fibres in combination with flax, hemp and glass fibres. Basalt revealed a higher resistance to deformation than other fibre types in the hybrids. On the other side, it was also evidenced that the mechanical properties of basalt reinforced composites are significantly influenced by the matrix used to fabricate them [31].

In general terms, as illustrated above, basalt fibre composites may compare well with E-glass fibre ones as far as mechanical and impact performance is concerned. However, the suitability of basalt fibre in filament winding process and the response under impact of filament wound structures based on basalt fibres underwent limited investigations so far. Therefore, the aim of this investigation is to determine the

capability of basalt tubes to withstand falling weight impact, evaluating their performance and comparing it with that of E-glass tubes in terms of winding angle, energy level and different impactor geometrical sizes.

2. EXPERIMENTAL

2.1 Materials and Methods

Basalt roving of 2400 Tex, with average filament diameter of 22 microns, was purchased from Incotelogy GmbH company, located in Pulheim, Germany, while E-glass and carbon roving fibres with the same linear density (with average filament diameter of 17 microns and 7 microns, respectively) were supplied from Universal Star Group Limited Company in Ningbo, China. Epoxy resin was purchased from S&N Chemical Company, located in Johor, Malaysia. Dry filament winding process with angles (α), $[\pm 45^0]_3$, $[\pm 55^0]_3$, $[\pm 65^0]_3$ and $[\pm 75^0]_3$ were used in this study for basalt tubes (B45, B55, B65 and B75), prior to subsequent process. The measurement of winding angle (α), as shown in Figure 1, and specifications on dry winding process in Table 1, were both obtained from simulation program using Cadwind V9 software.

Vacuum infusion process (VIP) was used to impregnate the fibre using epoxy 1006 resin, as well as to control the quality of fabrication for all samples. Since density of both fibre and resin are not verified independently, it is not strictly accurate to use the constituent densities to obtain fibre volume fraction FVF, although this might serve as a first approximation for this measurement. The electronic densimeter is used to determine the density of the whole composite specimen, taking as reference densities 2.55 g/cm³ for glass, 2.7 g/cm³ for basalt and 1.15 g/cm³ for epoxy resin. On the other side, burn-off test was used to identify the weight fraction of fibres. The standard

methods for density and weight fraction are referred to ASTM D792, and ASTM D2584 respectively, and they were used for calculating the volume fraction of fibres using Equation 1 as follows [33,34]:

$$Fibre\ Volume\ Fraction, FVF = \frac{\rho_c W_f}{\rho_f W_c} \quad (1)$$

where density (ρ) and weight (W) of fibre (subscript f) and composite (subscript c) are involved in the equation to obtain FVF. This calculation refers to the densities of the single constituents, which are normally less sensitive to physical properties after void content measurement (ASTM D2734) [35]. Four different configurations of basalt tubes have been shown, and comparison between E-glass and carbon tubes has been performed on a single configuration, which is [±55°] winding angle. This has been selected due to optimum specification (lower percentage winding coverage) that indirectly can reduce the slippage effect during manufacturing process.

2.2 Impact testing

Impact tests were performed using the Instron Dynatup 8250 Drop Weight Impact Tester model that was supplied by Instron Company, Singapore branch. Different impact potential energies of 4, 6, 8 and 10 J were used towards basalt/epoxy filament wound tubes samples (length 150 mm, diameter 50 mm, 3 mm wall thickness) and the test was performed at room temperature with v-groove support fixture to hold the tubes sample. The height was the only variable input on this falling impact event and was used to control the potential energy during the experiment, as shown in Table 3. Contact force, deflection, energy absorption, velocity and time were automatically obtained

from the INSTRON Bluehill's software to describe the impact performance of the material. The test was also conducted using four impactors with different hemispherical tips with respective diameters 6.35, 10, 12.7 and 15.9 mm (D1, D2, D3 and D4), as shown in Figure 2. The maximum damage diameter (MDD) sizes were measured from the impacted sample, following indications from ASTM D7136-12 [36]. To obtain the MDD, the damage zone area is simply measured by positioning the string along the damage contour surface. The string was marked to obtain the exact length of damage and measured by a Vernier calliper.

3. RESULTS AND DISCUSSION

3.1 Impact Response

A series of tests with four impact energies, from 4 to 10 J, was selected to determine impact characteristics and damage patterns for basalt filament wound composite tubes. Low impact energies were purposely selected to concentrate on the advantages and drawbacks of basalt with respect to E-glass fibres, for filament wound tubes on which a limited amount of damage is produced. Five samples were tested for each category and a number of characteristics, including peak load, contact duration, absorbed energy and damage diameter were acquired from the impact event.

Transverse impact tests were performed on four different winding angles, namely $[\pm 45°]_3$, $[\pm 55°]_3$, $[\pm 65°]_3$ and $[\pm 75°]_3$, on the tubes with 50 mm diameter for 4 Joules of impact energy. Based on Figure 3 (a), the slope of the curve slightly increased in the initial quasi-linear part of the curve, in other words offering some increase to the linear stiffness angle as far as the winding angle is higher. It is likely that matrix cracking and delamination start occurring when the first load drop occurs, then these damage

phenomena become more frequent as far as the maximum contact force is reached. It can be noticed that this force increases the wider the winding angle. As from the filament winding process, a different amount of fibre is used for each angle: in practice, a decreasing winding angle leads to the increase of amount of fibres used (Table 1). It is found that the different distribution of fibres obtained with higher winding angles has some positive effect on tubes' rigidity and also on the extent of impact damage, despite the fact that the amount of fibre introduced is lower as shown in Table 4. In practice, B75 tubes have the lowest deflection value in their response to impact loads, therefore suggesting that damage is more spread over the tube surface therefore reducing the depth of penetration [2]. The effect of winding angle over the surface distribution of damage will be discussed also further down. The peak force and damage depth of basalt tubes increases with growing impact energy, so that in practice the total deflection of the tubes have an around 1.5 mm relative difference between the highest and the lowest energy level conditions at 55° winding angle, which have been represented in Figure 3(b).

Figure 4 shows the absorbed energy values of basalt tubes with four different winding angles. As mentioned, when the winding angle decreases due to the percentage of covering requirement, more fibres are required, which in principle would lead the tubes to become stiffer [38]. In contrast, what is observed is that the higher the winding angle for basalt tubes the higher also their elastic stiffness, as from Table 4. This might be possibly due to a different distribution of damage over their structure, especially at the higher energy level.

On the other side, the slightly higher amount of fibres introduced would possibly bring tubes with lower winding angle to offer improved impact energy absorption capability. Dissipation is minimal for impact at 4 J, as suggested in Figure 5 (a), for basalt and even more so for E-glass tubes, and virtually non existent for carbon fibre ones, thus indicating their brittleness. In contrast, the brittleness of carbon fibre led to major damage, indicated by the full penetration of the impactor in the tubes [37]. Also, basalt tubes are slightly superior in terms of impact to E-glass ones, as suggested also in [6, 18]: here this is confirmed, though with very small differences, as reported from head to head comparison in Figure 5(b). The comparisons were made based on the same configuration in which the fibre amount, fibre direction and impregnation process are strictly controlled through the same procedure. The impact resistance depends on the characteristics of the reinforcement material, its interaction with epoxy matrix and the suitability of the winding process: however, as a whole, due to the mode of penetration and to the quite low thickness involved, it can be suggested that BVID threshold is very low, since already at 4 J all samples show some damage.

Damage resistance properties are highly dependent on several factors including impactor geometry [4]. A series of tests using four impactor diameter sizes was performed to determine the impact characteristics and damage patterns for basalt filament wound composite tubes. Hemispherical strikers with four different diameter sizes have been used on basalt tubes: D1 (6.35 mm), D2 (10 mm), D3 (12.7 mm) and D4 (15.9 mm). D3 offered the higher elastic linear stiffness, calculated as the average slope of the quasi-elastic part of the impact hysteresis cycle, normally up to the peak load [39] (Table 5) and peak load values, which revealed the decreasing results as the

impactor size is also reduced, as shown in Figure 6(a). Smaller sizes of impactor recorded high deflection value of almost 2 mm differences when compared to larger impactor sizes. The deeper penetration by a smaller impactor represents a high localized concentration on the impact location [4]. The correlation between winding angles and impactor sizes has been illustrated in Figure 6(b). The decreasing patterns were observed consistently, when the winding angle of the basalt tubes increases.

3.2 Impact Damage

Figure 7 shows the images of basalt composite tubes impacted under different impact energy. Based on observation, it can be seen that higher impacted energy produced a higher damage area. The impacted basalt tubes show good resistance to impact loads where it is representing flexible characteristics due to a smaller amount of energy dispersion on the tubes surface [2].

The maximum damage diameter (MDD), as from images taken from the impacted samples, was found to be reduced when the winding angle increases, as shown in Figure 8. More into detail, it was also revealed that passing from 4 to 10 Joules impact energy, MDD results show a very large variation for basalt fibre tubes with ±45° winding angle, while gradually more limited differences were encountered for larger winding angles. It can be suggested that ±45° basalt tubes, together with slightly lower rigidity, present a higher sensitivity to the presence of damage and an increased difficulty to accommodate it. In the case of highest winding angle applied, ±75° tubes, it can be suggested that not much difference is present among impact damage areas at different energies, except for the maximum energy applied, 10 J. This might imply that the structure is capable to

somehow accommodate some damage, although the rate of damage propagation is more difficult to predict, as it is very far from linearity, possibly as the effect of many manufacturing parameters involved, such as winding angle, winding pattern and build-in thickness [40, 41].

The significant difference of the damage zone area between E-glass and basalt tubes for impact at 10 J has been shown in Figure 9: here, E-glass tubes appear to dissipate more energy in terms of delamination if compared to basalt tubes. Comparison data between basalt and E-glass tubes as regards MDD is depicted in Figure 10, as the function of the winding angle on different energy levels. Tubes with different winding angles were compared: and those with ±75° winding angle exhibited the least damaged area for both basalt and E-glass tubes, although on very different levels.

The size of the hemispherical tip diameter influences the damaged area on the basalt tubes: the likely situation is that the damaged area will grow with the impactor diameter: however, as always, there is no linearity in this increase and this is further complicated by the effect of a winding angle. On the other side, shallower penetration of damage as the result of the use of a larger impactor sizes results in a wider damaged area due to a global response rather than a high localized stress concentration in that particular area [4]. The correlation between MDD and winding angles can be seen in Figure 11 where basalt tubes with ±75° winding angles experienced a lower amount of damage using all sizes of impactors when compared to other tube angles. The comparison between E-glass and basalt fibre laminates, which can be observed in Figure 12, indicated that both basalt and E-glass tubes were affected directly by the

variation in impactor diameter. However, larger impactors generated impacts of more circular shape, particularly on E-glass fibre tubes, less so on basalt fibre ones. It can be possibly suggested therefore that a larger contact surface with the impactor would reduce the effect of crossovers, which is mainly related to the mutual slippage between fibres, although partially hindered by the polymer matrix [42]. More slippage should be related with an increased directionality of damage, in the direction of fibres: in other words, it is likely that using smaller impactors directional cracks are more easily produced. Moreover, the effect of tube curvature is less affected by the local characteristics of the woven fibres (e.g., crossovers) in the composite: this is particularly the case in damage produced by the largest size impactor (D4). In term of comparison between tubes, E-glass fibre composites absorbed more energy through delamination, as reported before, possibly for a more gradual process of fibre-matrix interface failure.

A high localized stress concentration induced by a smaller impactor created a deeper penetration [4]. Therefore, less damage occurred from the impact load. Less energy is required to extend the delamination in the longitudinal direction due to restricted movement by the borders in the circumferential direction [2]. Comparisons between basalt and E-glass fibre composite laminates revealed significant differences. It can be seen that E-glass tubes produced a larger damaged area indicating the presence of equally larger delaminated areas. It has been reported elsewhere that the major mode for impact damage absorption in basalt fabrics composites appears to be fibre breakage with delamination appearing less diffuse than in E-glass fibre composites [20].

As far as impact strength is concerned, E-glass tubes absorbed more impact energy, as supported by results in Figure 5. The details of the MDD results have been illustrated in

Figure 13 where a head to head comparison has been done on different impactor sizes involving two different materials.

As regards the surface morphology, matrix cracking and fibre pullout can easily be observed in Figure 14 referring to the minimal energy case for the ±55° filament wound tubes. Impact on basalt tubes created particularly significant matrix cracking and fibre fracture due to energy concentration in that particular area. The delamination is the indicator of dissipation of impact energy, and the separation of layers has been focused on in the SEM micrographs. Images at three different magnifications, namely x100, x250 and x500, were obtained from SEM, which illustrated the area of the damaged zone in basalt composite tubes. The comparison has been made between E-glass and carbon tubes under the same impact energy, as reported in Figure 15. The E-glass tubes suffered permanent damage where fibre pullout occurred in the matrix cracking region, while damage in basalt fibre tube appears more concentrated and with more limited pullout. It may be concluded that the use of basalt fibre for filament wound tubes offers better damage resistance, at the expense of some weight penalty, offers more controllable damage morphology with respect to E-glass and carbon fibre composite tubes.

4. CONCLUSIONS

Based on this study, effects of transverse impact load on basalt filament wound tubes were observed, in particular varying three parameters, winding angle of the tubes, impact energy and hemispherical tip impactor diameter.

The main conclusions drawn from this investigation are as follows:

- Maximum contact force increases the higher the impact energy for basalt tubes while it does not change significantly for different winding angles.
- Maximum damage diameter (MDD) of basalt tubes obviously increases the higher the impact energy, but with not very predictable patterns, also because the shape of damaged area changes with it. It also increases with the higher winding angles.
- Basalt tubes with higher winding angles tend to absorb less energy than the tubes with smaller winding angles for any given impact energy, which may be also the effect of them being slightly thinner.
- Impact damage typically propagates in the fibre direction of the tubes. By increasing the impactor diameter the damage area centred in the point of impact becomes larger, hence reducing the penetration. The damage area on basalt tubes appears significantly smaller than in E-glass tubes with similar amount of reinforcement at all impact energies. However, a fully reliable comparison would require having laminates with very close thicknesses, which was technically not feasible for the different fibres and in the case of basalt for the different winding angles adopted.

Therefore, the outcome for this research can be useful as guidance for producing alternative tubular structure for load bearing application, hence reducing the dependency to metallic and synthetic reinforcement materials, such as carbon and E-glass, therefore potentially increasing their sustainability.

ACKNOWLEDGEMENTS

The financial support from Research University Grant (RUG) UTM Malaysia (Vot:Q.J130000.2509.07H64) to develop present research work. The Centre for Composites (CfC) and Marine Technology Centre (MTC) of University Teknologi Malaysia for providing the facilities and School of Architecture and Design of Università degli Studi di Camerino for consultancy support.

REFERENCES

1. Minak, G., Abrate, S., Ghelli, D., Panciroli, R., & Zucchelli, A. (2010). Low-velocity impact on carbon/epoxy tubes subjected to torque–experimental results, analytical models and FEM analysis. *Composite Structures*, 92(3), 623-632.
2. Deniz, M. E., Karakuzu, R., Sari, M., & Icten, B. M. (2012). On the residual compressive strength of the glass–epoxy tubes subjected to transverse impact loading. *Journal of Composite Materials*, 46(6), 737-745.
3. Deniz, M. E., & Karakuzu, R. (2012). Seawater effect on impact behavior of glass–epoxy composite pipes. *Composites Part B: Engineering*, 43(3), 1130-1138.
4. Chib, A. (2006). Parametric study of low velocity impact analysis on composite tubes (PhD dissertation, Wichita State University). Available online at: http://soar.wichita.edu/xmlui/bitstream/handle/10057/267/t06004.pdf (accessed 9th December 2015)
5. Doyum, A. B., & Altay, B. (1997). Low-velocity impact damage in glass fibre/epoxy cylindrical tubes. *Materials & Design*, 18(3), 131-135.
6. Deák, T., & Czigány, T. (2009). Chemical composition and mechanical properties of basalt and glass fibers: a comparison. *Textile Research Journal*, 79(7), 645-651.

7. Dorigato, A., & Pegoretti, A. (2014). Flexural and impact behaviour of carbon/basalt fibers hybrid laminates. *Journal of Composite Materials*, 48(9), 1121-1130.
8. Colombo, C., Vergani, L., & Burman, M. (2012). Static and fatigue characterisation of new basalt fibre reinforced composites. *Composite Structures*, 94(3), 1165-1174.
9. Carmisciano, S., De Rosa, I. M., Sarasini, F., Tamburrano, A., & Valente, M. (2011). Basalt woven fiber reinforced vinylester composites: Flexural and electrical properties. *Materials & Design*, 32(1), 337-342.
10. Manikandan, V., Jappes, J. W., Kumar, S. S., & Amuthakkannan, P. (2012). Investigation of the effect of surface modifications on the mechanical properties of basalt fibre reinforced polymer composites. *Composites Part B: Engineering*, 43(2), 812-818.
11. Cerny, M., Glogar, P., & Sucharda, Z. (2009). Mechanical properties of basalt fiber reinforced composites prepared by partial pyrolysis of a polymer precursor. *Journal of Composite Materials*, 43(9), 1109-1120.
12. Liu, Q., Shaw, M. T., Parnas, R. S., & McDonnell, A. M. (2006). Investigation of basalt fiber composite mechanical properties for applications in transportation. *Polymer Composites*, 27(1), 41-48.
13. Kim, M. T., Rhee, K. Y., Park, S. J., & Hui, D. (2012). Effects of silane-modified carbon nanotubes on flexural and fracture behaviors of carbon nanotube-modified epoxy/basalt composites. *Composites Part B: Engineering*, 43(5), 2298-2302.
14. Szabó, J. S., & Czigány, T. (2003). Static fracture and failure behavior of aligned discontinuous mineral fiber reinforced polypropylene composites. *Polymer Testing*, 22(6), 711-719.

15. Czigány, T. (2006). Special manufacturing and characteristics of basalt fiber reinforced hybrid polypropylene composites: mechanical properties and acoustic emission study. *Composites Science and Technology*, 66(16), 3210-3220.
16. Zhang, Y., Yu, C., Chu, P. K., Lv, F., Zhang, C., Ji, J., & Wang, H. (2012). Mechanical and thermal properties of basalt fiber reinforced poly (butylene succinate) composites. *Materials Chemistry and Physics*, 133(2), 845-849.
17. Akinci, A., Yilmaz, S., & Sen, U. (2012). Wear behavior of basalt filled low density polyethylene composites. *Applied Composite Materials*, 19(3-4), 499-511.
18. Lopresto, V., Leone, C., & De Iorio, I. (2011). Mechanical characterisation of basalt fibre reinforced plastic. *Composites Part B: Engineering*, 42(4), 717-723.
19. Dehkordi, M. T., Nosraty, H., Shokrieh, M. M., Minak, G., & Ghelli, D. (2010). Low velocity impact properties of intra-ply hybrid composites based on basalt and nylon woven fabrics. *Materials & Design*, 31(8), 3835-3844.
20. De Rosa, I. M., Marra, F., Pulci, G., Santulli, C., Sarasini, F., Tirillò, J., & Valente, M. (2011). Post-impact mechanical characterisation of E-glass/basalt woven fabric interply hybrid laminates. *Express Polymer Letters*, 5(5), 449-459.
21. De Rosa, I. M., Marra, F., Pulci, G., Santulli, C., Sarasini, F., Tirillò, J., & Valente, M. (2012). Post-impact mechanical characterisation of glass and basalt woven fabric laminates. *Applied Composite Materials*, 19(3-4), 475-490.
22. Wang, X., Hu, B., Feng, Y., Liang, F., Mo, J., Xiong, J., & Qiu, Y. (2008). Low velocity impact properties of 3D woven basalt/aramid hybrid composites. *Composites Science and Technology*, 68(2), 444-450.
23. Sarasini, F., Tirillò, J., Valente, M., Valente, T., Cioffi, S., Iannace, S., & Sorrentino, L. (2013). Effect of basalt fiber hybridization on the impact behavior

under low impact velocity of glass/basalt woven fabric/epoxy resin composites. *Composites Part A: Applied Science and Manufacturing*, 47, 109-123.

24. Dehkordi, M. T., Nosraty, H., Shokrieh, M. M., Minak, G., & Ghelli, D. (2013). The influence of hybridization on impact damage behavior and residual compression strength of intraply basalt/nylon hybrid composites. *Materials & Design*, 43, 283-290.
25. Sarasini, F., Tirillò, J., Valente, M., Ferrante, L., Cioffi, S., Iannace, S., & Sorrentino, L. (2013). Hybrid composites based on aramid and basalt woven fabrics: impact damage modes and residual flexural properties. *Materials & Design*, 49, 290-302.
26. Czigany, T., Pölöskei, K., & Karger-Kocsis, J. (2005). Fracture and failure behavior of basalt fiber mat-reinforced vinylester/epoxy hybrid resins as a function of resin composition and fiber surface treatment. *Journal of Materials Science*, 40(21), 5609-5618.
27. Mingchao, W., Zuoguang, Z., Yubin, L., Li, M., & Sun, Z. (2008). Chemical durability and mechanical properties of alkali-proof basalt fiber and its reinforced epoxy composites. *Journal of Reinforced Plastics and Composites*, 27(4), 393-407.
28. Sfarra, S., Ibarra-Castanedo, C., Santulli, C., Paoletti, A., Paoletti, D., Sarasini, F., & Maldague, X. (2013). Falling weight impacted glass and basalt fibre woven composites inspected using non-destructive techniques. *Composites Part B: Engineering*, 45(1), 601-608.
29. Gideon, R. K., Hu, H., Wambua, P., & Gu, B. (2014). Characterizations of basalt unsaturated polyester laminates under static three-point bending and low-velocity impact loadings. *Polymer Composites*, 35(11), 2203-2213.

30. Petrucci, R., Santulli, C., Puglia, D., Nisini, E., Sarasini, F., Tirillò, J., & Kenny, J. M. (2015). Impact and post-impact damage characterisation of hybrid composite laminates based on basalt fibres in combination with flax, hemp and glass fibres manufactured by vacuum infusion. *Composites Part B: Engineering*, 69, 507-515.
31. Czigány, T. (2004). Basalt fiber reinforced hybrid polymer composites. *In Materials Science Forum* 473, 59-66.
32. Liu, Q., Shaw, M. T., Parnas, R. S., & McDonnell, A. M. (2006). Investigation of basalt fiber composite aging behavior for applications in transportation. *Polymer Composites*, 27(5), 475-483.
33. ASTM D792. (2013). Standard Test Methods for Density and Specific Gravity (Relative Density) of Plastics by Displacement. *ASTM International*, West Conshohocken, PA, DOI: 10.1520/D0792, www.astm.org.
34. ASTM D2584. (2011). Standard Test Method for Ignition Loss of Cured Reinforced Resins. *ASTM International*. West Conshohocken, PA, DOI: 10.1520/D2584-11, www.astm.org.
35. ASTM D2734. (2009). Standard Test Methods for Void Content of Reinforced Plastics. *ASTM International*. West Conshohocken, PA, DOI: 10.1520/D2734-09, www.astm.org.
36. ASTM D7136/D7136M. (2012). Standard Test Method for Measuring the Damage Resistance of a Fiber-Reinforced Polymer Matrix Composite to a Drop-Weight Impact Event. *ASTM International*. West Conshohocken, PA, DOI: 10.1520/D7136_D7136M-12, www.astm.org.

37. Dorigato, A., & Pegoretti, A. (2014). Flexural and impact behaviour of carbon/basalt fibers hybrid laminates. *Journal of Composite Materials*, 48(9), 1121-1130.

38. Shibley, A. M. (1982). Filament winding. In Handbook of Composites (pp. 449-478). Springer US.

39. Santulli C (2003), Study of impact hysteresis curves on e-glass reinforced polypropylene laminates, Journal of Materials Science Letters 22 (22), 1557-1562.

40. Aslan, Z., Karakuzu, R., & Okutan, B. (2003). The response of laminated composite plates under low-velocity impact loading. *Composite Structures*, 59(1), 119-127.

41. Tarfaoui, M., Gning, P. B., Davies, P., & Collombet, F. (2007). Scale and size effects on dynamic response and damage of glass/epoxy tubular structures. *Journal of Composite Materials*, 41(5), 547-558.

42. Roylance, D (1980). Stress wave propagation in fibres: effect of crossovers, *Fibre Science and Technology* 13, 385-395.

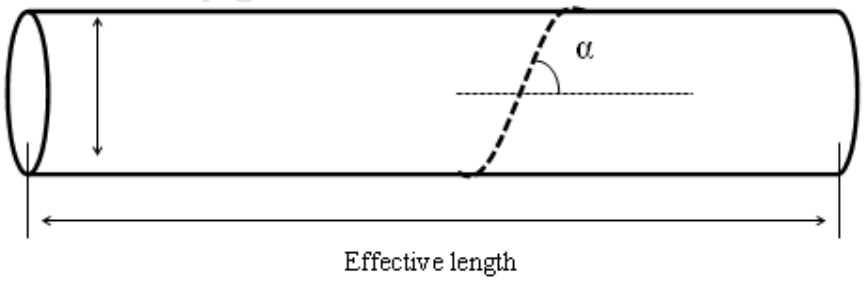

Figure 1: Schematic on winding tubes to determine winding angle (α)

Fibre roving	Winding angle (α)	Degree of covering (%)	Single laminate thickness (mm)	Fibre consumption (m)	Laminate weight, kg
Basalt	[±45°]	104	0.8439	79.83	0.25
	[±55°]	102	0.8336	72.15	0.23
	[±65°]	102	0.8252	69.35	0.22
	[±75°]	103	0.8228	68.20	0.22
E-glass	[±45°]	105	0.7990	79.83	0.25
	[±55°]	102	0.78761	72.15	0.23
	[±65°]	102	0.76985	69.35	0.22
	[±75°]	103	0.7710	68.20	0.21
Carbon	[±55°]	102	0.4342	72.15	0.15

Table 1: Basalt, E-glass and carbon fibre composite tubes specification on the dry filament winding process

Tubes	Thickness (mm)	Volume Fraction (approximated to the nearest %)
Basalt $[\pm 45^0]_3$	3.23 ± 0.04	55
Basalt $[\pm 55^0]_3$	3.19 ± 0.03	57
Basalt $[\pm 65^0]_3$	2.96 ± 0.03	55
Basalt $[\pm 75^0]_3$	2.81 ± 0.02	56
E-glass $[\pm 55^0]_3$	2.64 ± 0.04	56
Carbon $[\pm 55^0]_3$	1.24 ± 0.02	58

Table 2: Characteristics of basalt, E-glass and carbon fibre reinforced epoxy tubes (three layer laminate) produced by vacuum infusion process

Impact energy (Joules)	Velocity (m/s)	Duration (ms)	Total impacting weight (kg)	Height (m)
4	1.66	9.95	3	0.14
6	2.04	10.2	3	0.2
8	2.3	11.9	3	0.27
10	2.59	12.02	3	0.34

Table 3: Impact test configuration

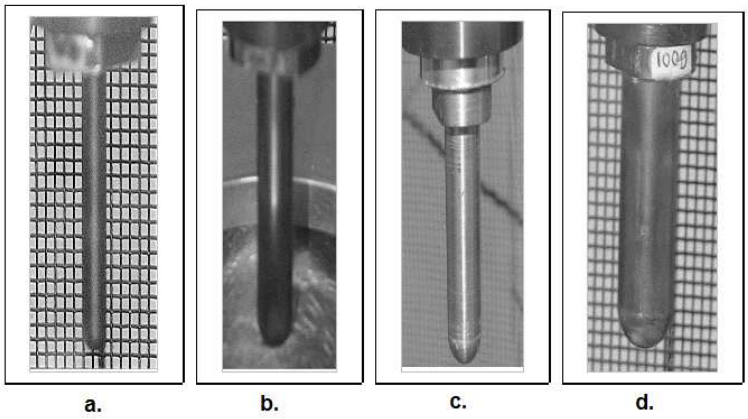

Figure 2: Different impactor sizes for impact test:

(a) 6.35mm, (b) 10mm, (c) 12.7mm and (d) 15.9mm

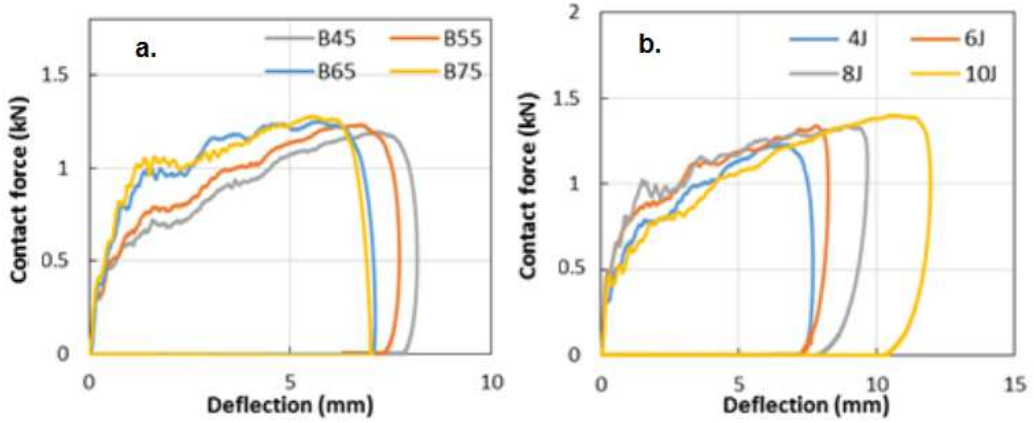

Figure 3: Evolution of impact load-deflection curves with (a) winding angle (4 J impact energy), and (b) impact energy (at 55° winding angle) (impactor diameter 6.35 mm)

Winding configuration	Elastic linear stiffness (kN/mm)
Basalt $[\pm 45^0]_3$	0.32 ± 0.02
Basalt $[\pm 55^0]_3$	0.34 ± 0.05
Basalt $[\pm 65^0]_3$	0.37 ± 0.05
Basalt $[\pm 75^0]_3$	0.41 ± 0.03
E-glass $[\pm 55^0]_3$	0.39 ± 0.04
Carbon $[\pm 55^0]_3$	0.24 ± 0.03

Table 4: Elastic linear stiffness from impact hysteresis cycles (energy=4 Joules) with different winding configurations and comparison with E-glass and carbon fibre composites (Impactor diameter 12.7 mm)

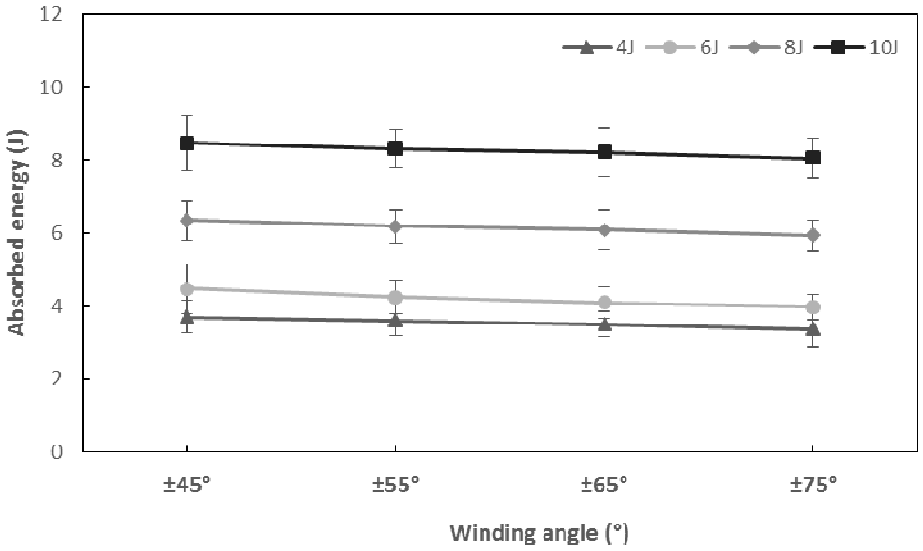

Figure 4: Absorbed energy vs. winding angle for basalt fibre composites impacted at different energies (impactor diameter 12.7 mm)

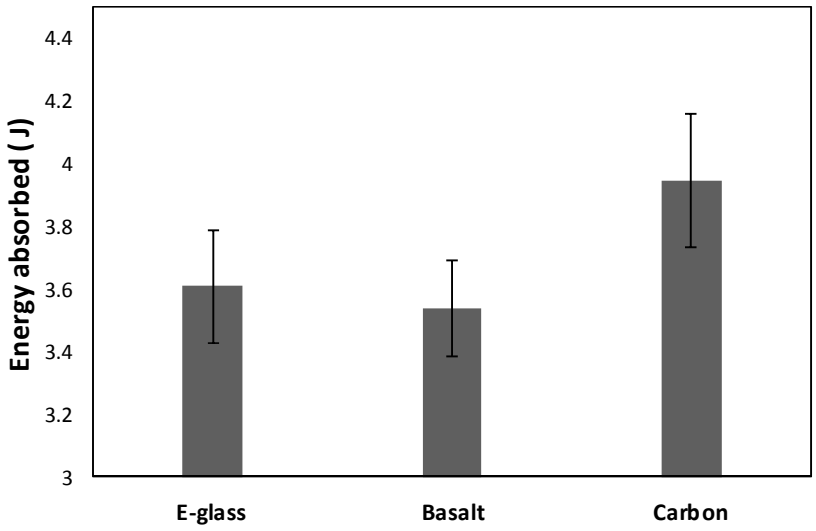

(a)

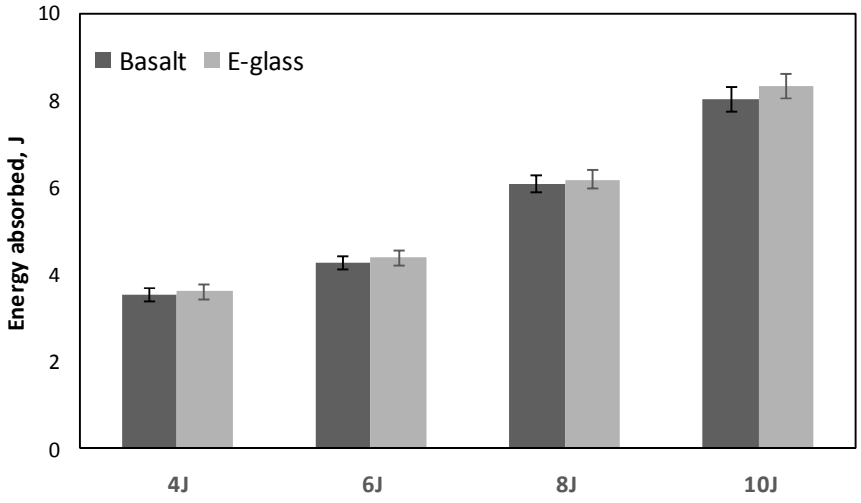

(b)

Figure 5: Energy absorption of composite tubes: (a) For 4 J impact energy, and (b) E-glass/basalt head-to-head comparison on ±55° winding angle (12.7 mm impactor diameter)

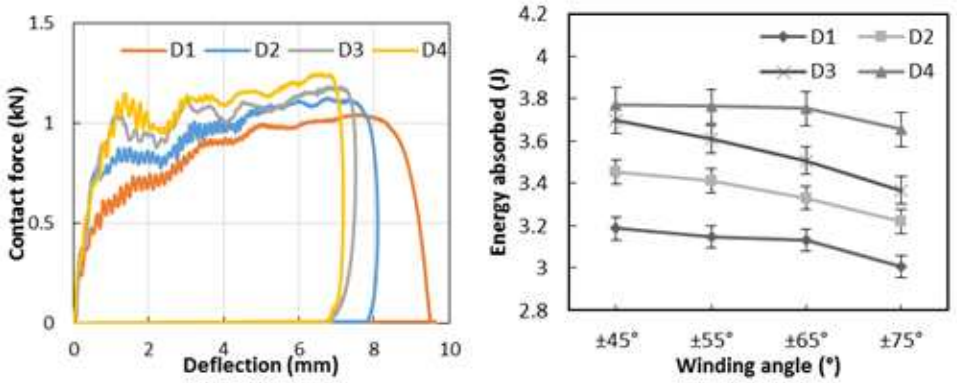

(a)

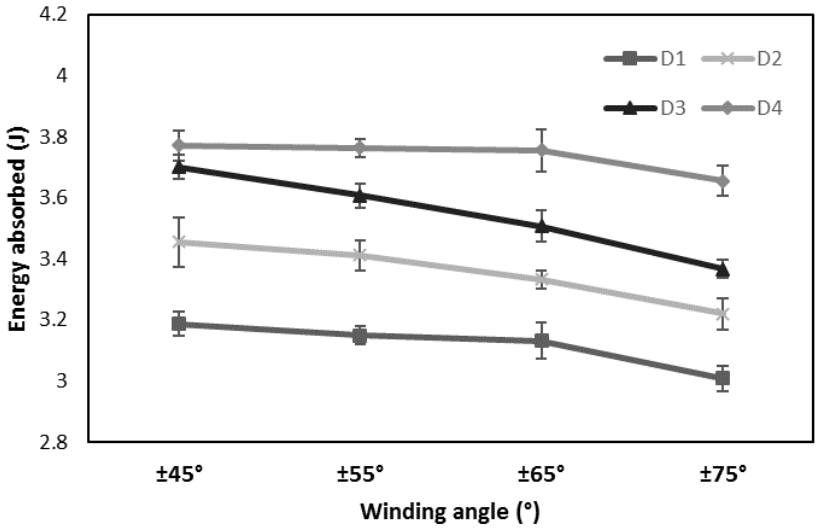

(b)

Figure 6: Typical response under different impactor sizes on basalt composite tubes:

(a) Contact force on ±55° winding angle,

(b) Energy absorbed on 4 J impact energy

Hemispherical impactor diameter (mm)	Elastic Linear Stiffness (kN/mm)
D1 (6.35)	0.26 ± 0.02
D2 (10)	0.32 ± 0.03
D3 (12.7)	0.41 ± 0.03
D4 (15.9)	0.33 ± 0.02

Table 5: Elastic linear stiffness from impact hysteresis cycles with different impactor sizes on ±55°winding angle (Impact energy = 10 Joules)

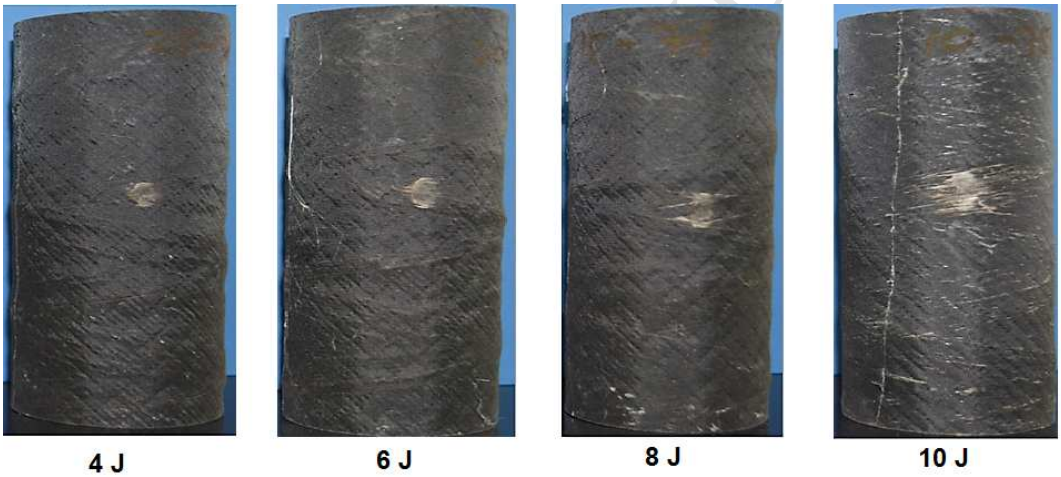

Figure 7: Images of impacted basalt composite tubes at different impact energies (impactor diameter size 12.7 mm) on ±75° winding angle

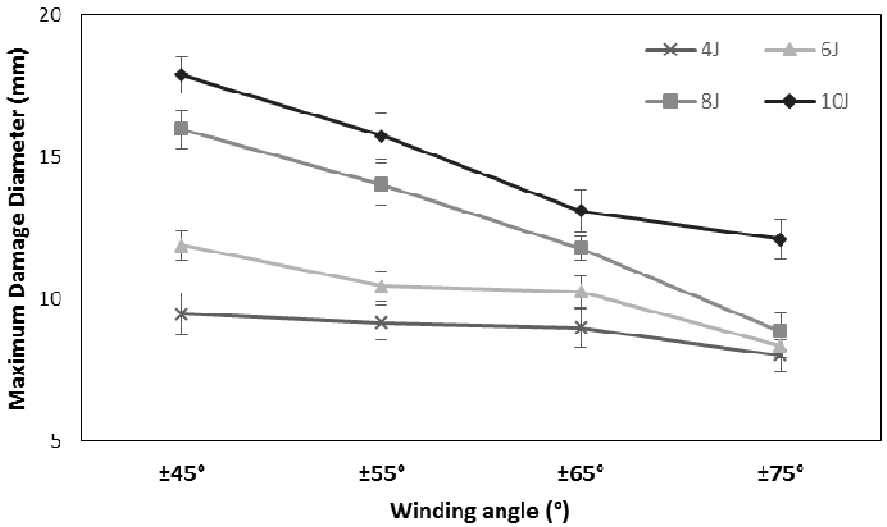

Figure 8: Comparison of maximum damage diameters (MDD) of basalt composite tubes for different impact energies and winding angles (impactor diameter 12.7 mm)

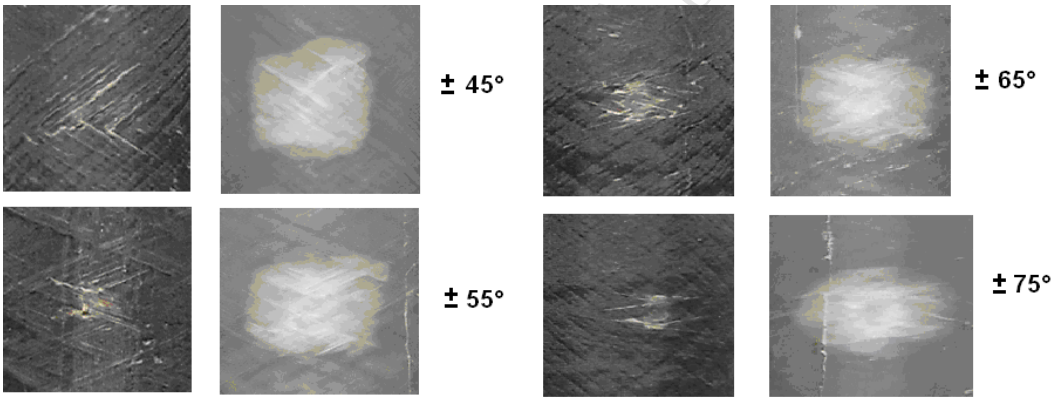

Figure 9: Compared images of basalt and E-glass tubes with different winding angles impacted at 10 J (impactor diameter 12.7 mm)

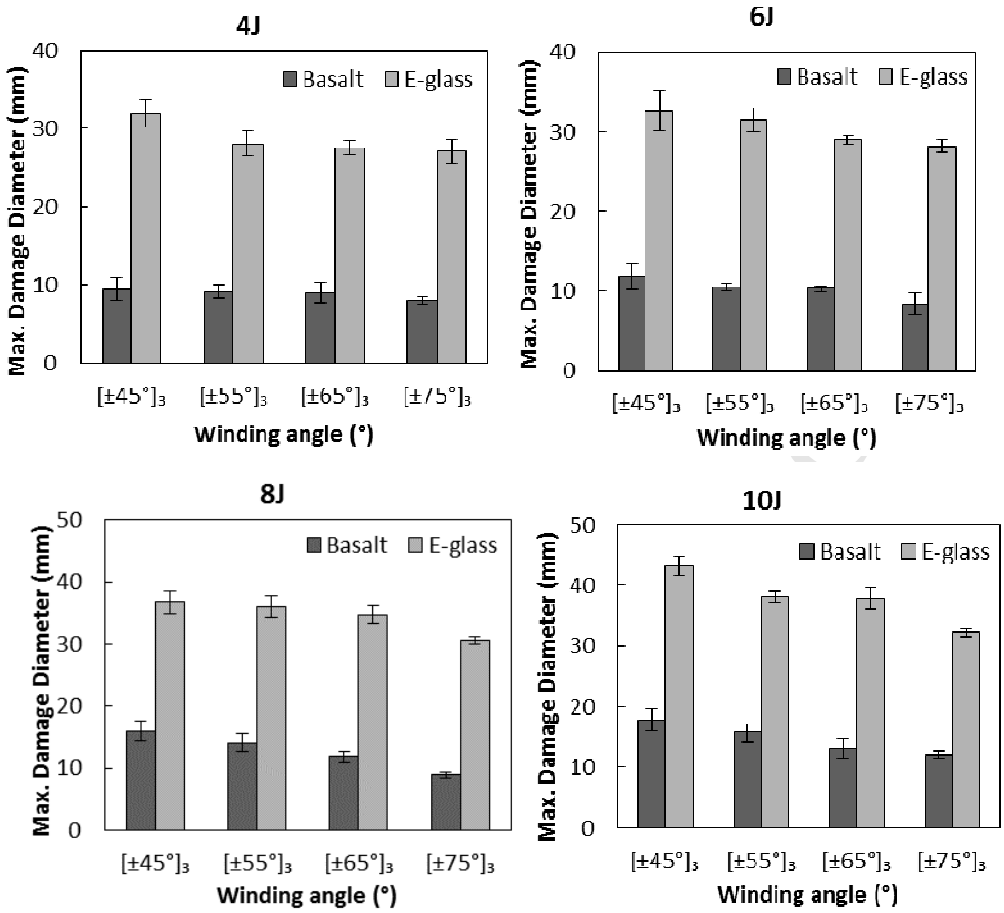

Figure 10: Comparison of maximum damaged diameters of basalt and E-glass tubes for different impact energies and winding angles (impactor diameter 12.7 mm)

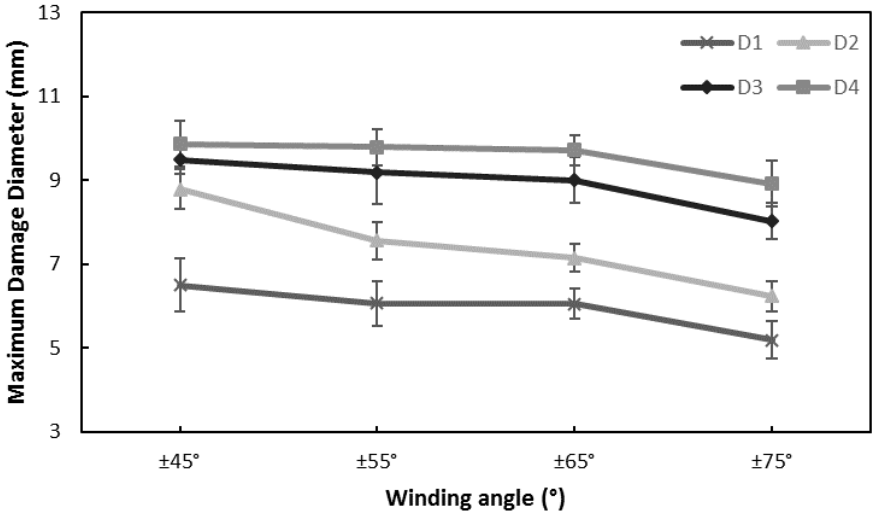

Figure 11: Comparison of maximum damaged diameters of basalt composite tubes for different impactor sizes for 4 joules impact energy.

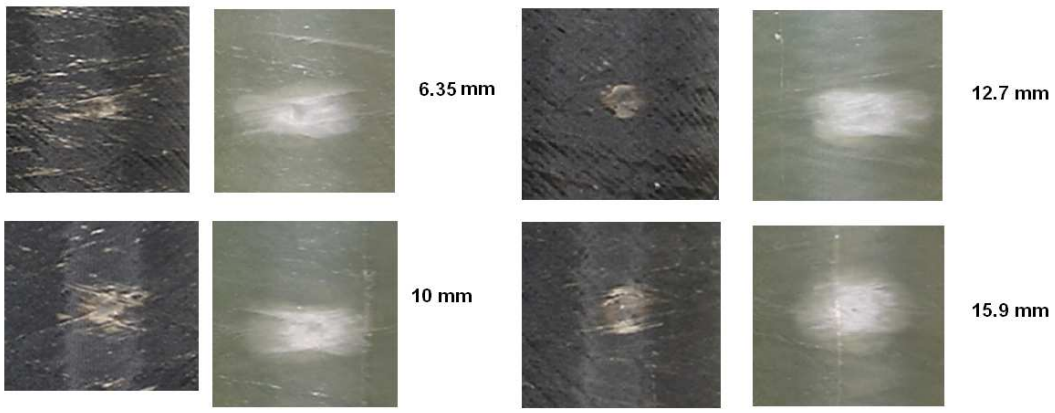

Figure 12: Comparison **i**mages of damage on 4 Joules impacted ±75° basalt and E-glass tubes at different impactor sizes

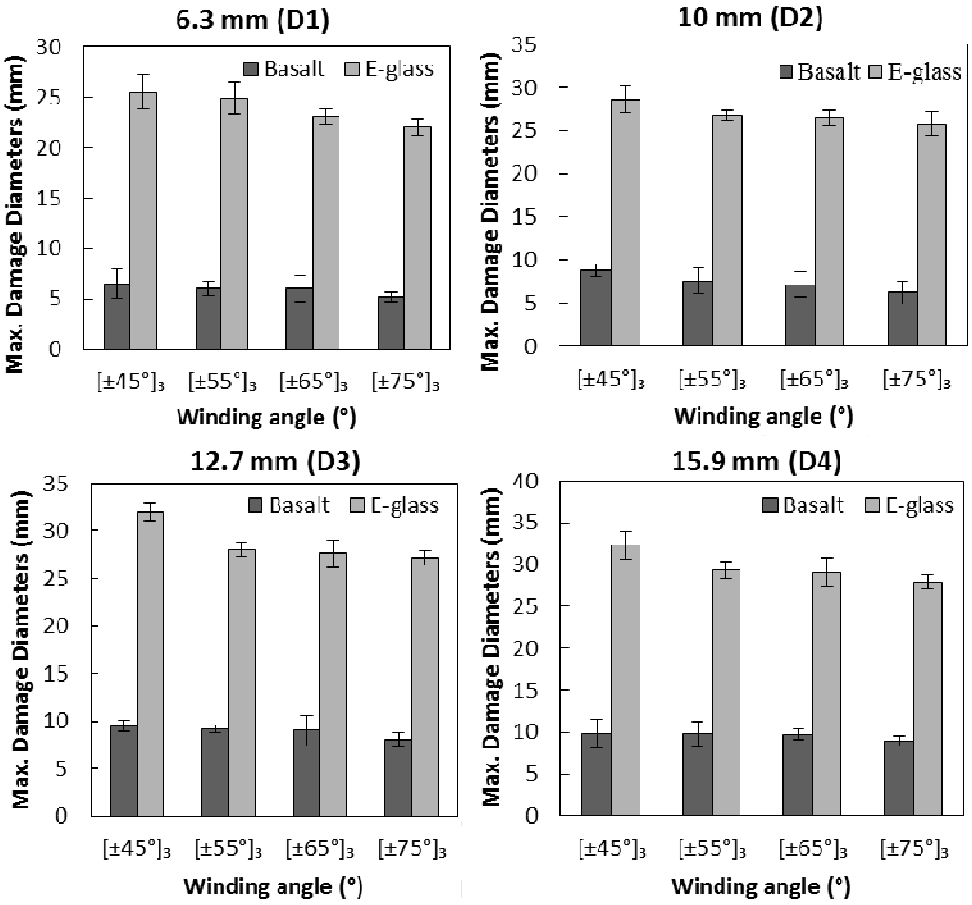

Figure 13: Comparison of maximum damaged diameters of basalt and E-glass tubes for different impactor sizes and winding angles at 4 joules impact energy

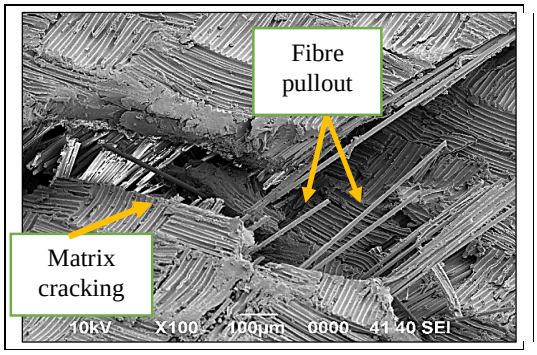

(a) 100x

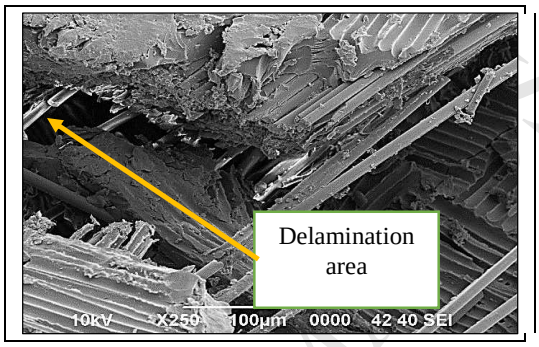

(b) 250x

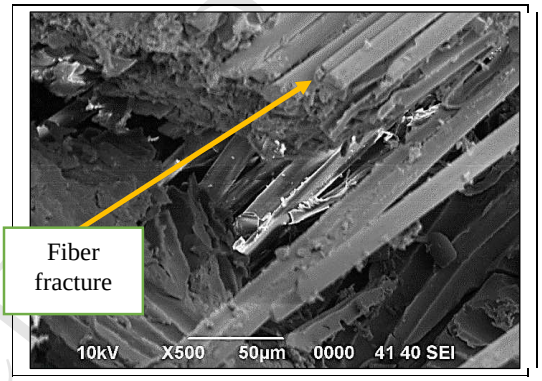

(c) 500x

Figure 14: Surface damage of basalt composite tubes under impact load (10J with 12.7 mm impactor on a ±55° tube): (a) 100x, (b) 250x and (c) 500x SEM magnification

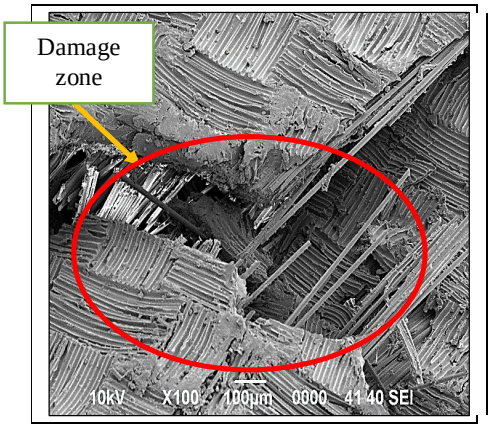

(a) Basalt

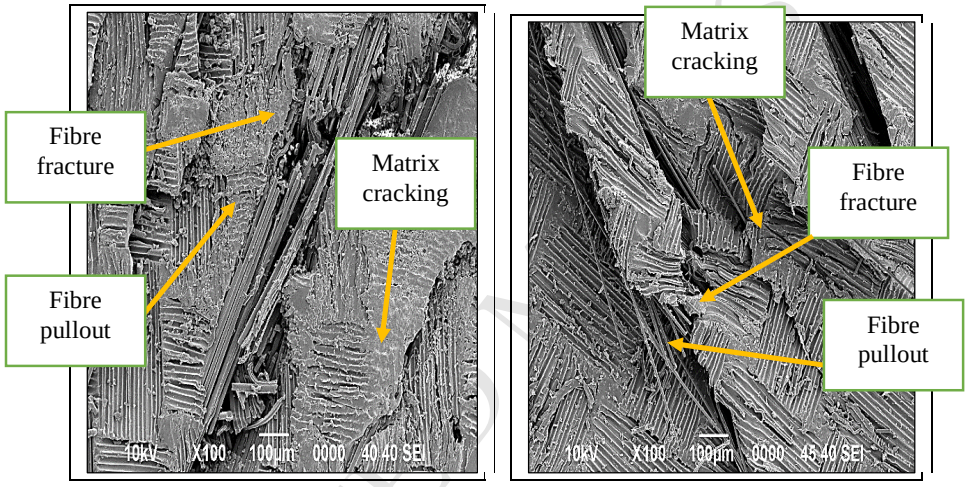

(b) E-glass (c) Carbon

Figure 15: Comparison of surface damage on tubes with different materials (impact at 10 J on ±55° filament wound tubes with impactor of 12.7 mm diameter)